SUPPLEMENTARY FIGURES

for

Combined Targeting of G9a and Checkpoint kinase 1 Synergistically Inhibits Pancreatic Cancer Cell Growth by Replication Fork Collapse

Guillermo Urrutia[1], Ann Salmonson[1], Jorge Toro-Zapata[1], Thiago M. de Assuncao[1,3], Angela Mathison[1,3], Nelson Dusetti[2], Juan Iovanna[2], Raul Urrutia[1,3,4], and Gwen Lomberk[1,3,5]

[1]Division of Research, Department of Surgery; Medical College of Wisconsin, 8701 Watertown Plank Road, Milwaukee, Wisconsin, 53226, USA.

[2]Centre de Recherche en Cancérologie de Marseille (CRCM), INSERM U1068, CNRS UMR 7258, Aix-Marseille Université and Institut Paoli-Calmettes, Parc Scientifique et Technologique de Luminy, 163 Avenue de Luminy, 13288 Marseille, France.

[3]Genomic Sciences and Precision Medicine Center (GSPMC), Medical College of Wisconsin, 8701 Watertown Plank Road, Milwaukee, Wisconsin, 53226, USA.

[4]Department of Biochemistry, Medical College of Wisconsin, 8701 Watertown Plank Road, Milwaukee, Wisconsin, 53226, USA.

[5]Department of Pharmacology and Toxicology, Medical College of Wisconsin, 8701 Watertown Plank Road, Milwaukee, Wisconsin, 53226, USA.

Corresponding author: Gwen Lomberk, PhD; Medical College of Wisconsin, TBRC 4860, 8701 Watertown Plank Road, Milwaukee, Wisconsin, 53226, USA; Tel: 1-414-955-2440; email: glomberk@mcw.edu

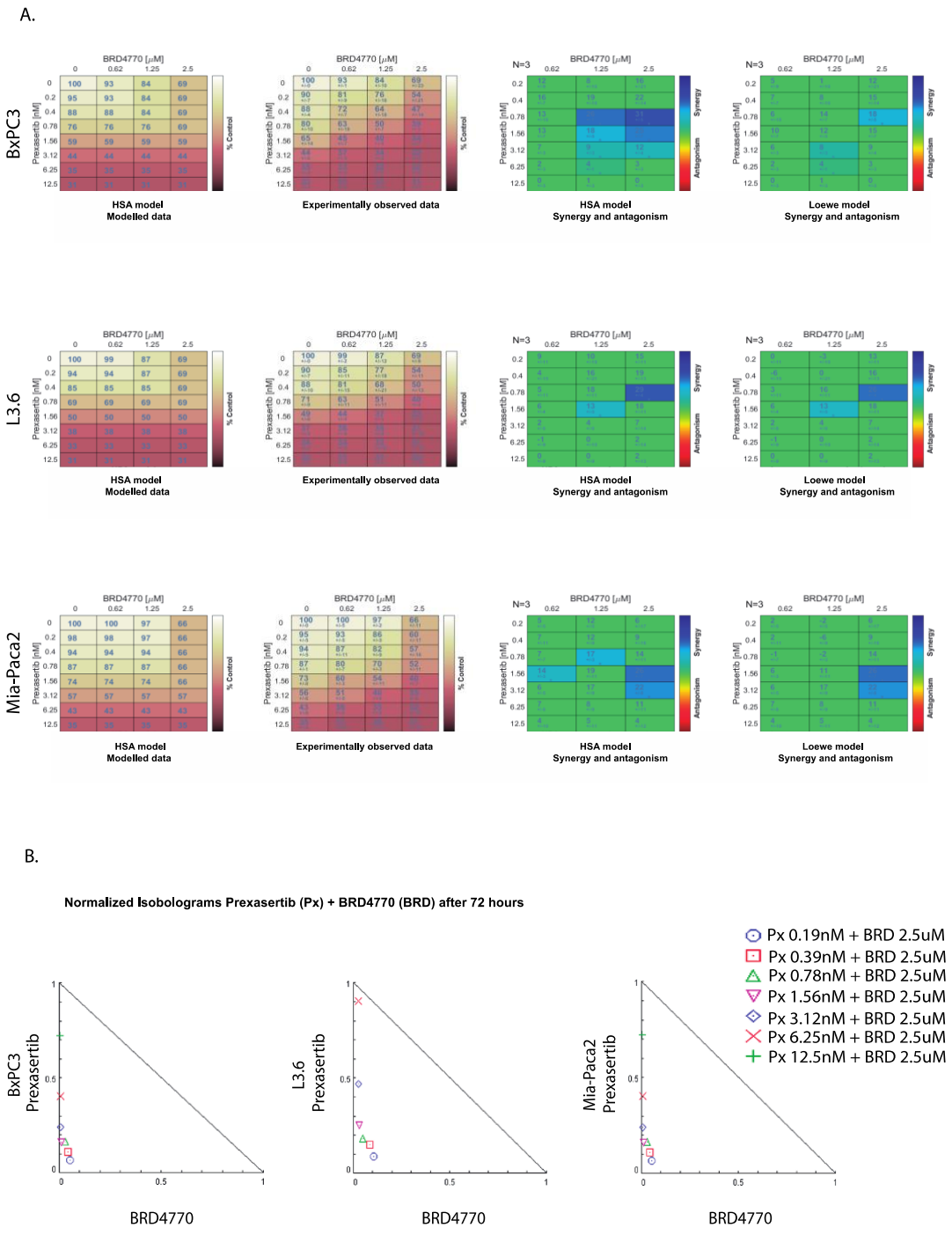

Supplementary Figure 1. Prexasertib and BRD4770 synergistically inhibit cell growth in PDAC cell lines. A, BxPC3, L3.6 and MiaPaca2 were treated with Prexasertib and BRD4770 in an 8x4 concentration grid for 72hrs. Modelled and experimental data (first and second panels from left to right) were analyzed independently with the HSA and Loewe synergy models (third and fourth panels) using Combenefit. **B,** Calculated isobolograms using Compusyn software are also shown for the combined treatment of prexasertib (Px; various doses as indicated) with BRD4770 (2.5µM) after 72hrs, confirming a synergistic interaction.

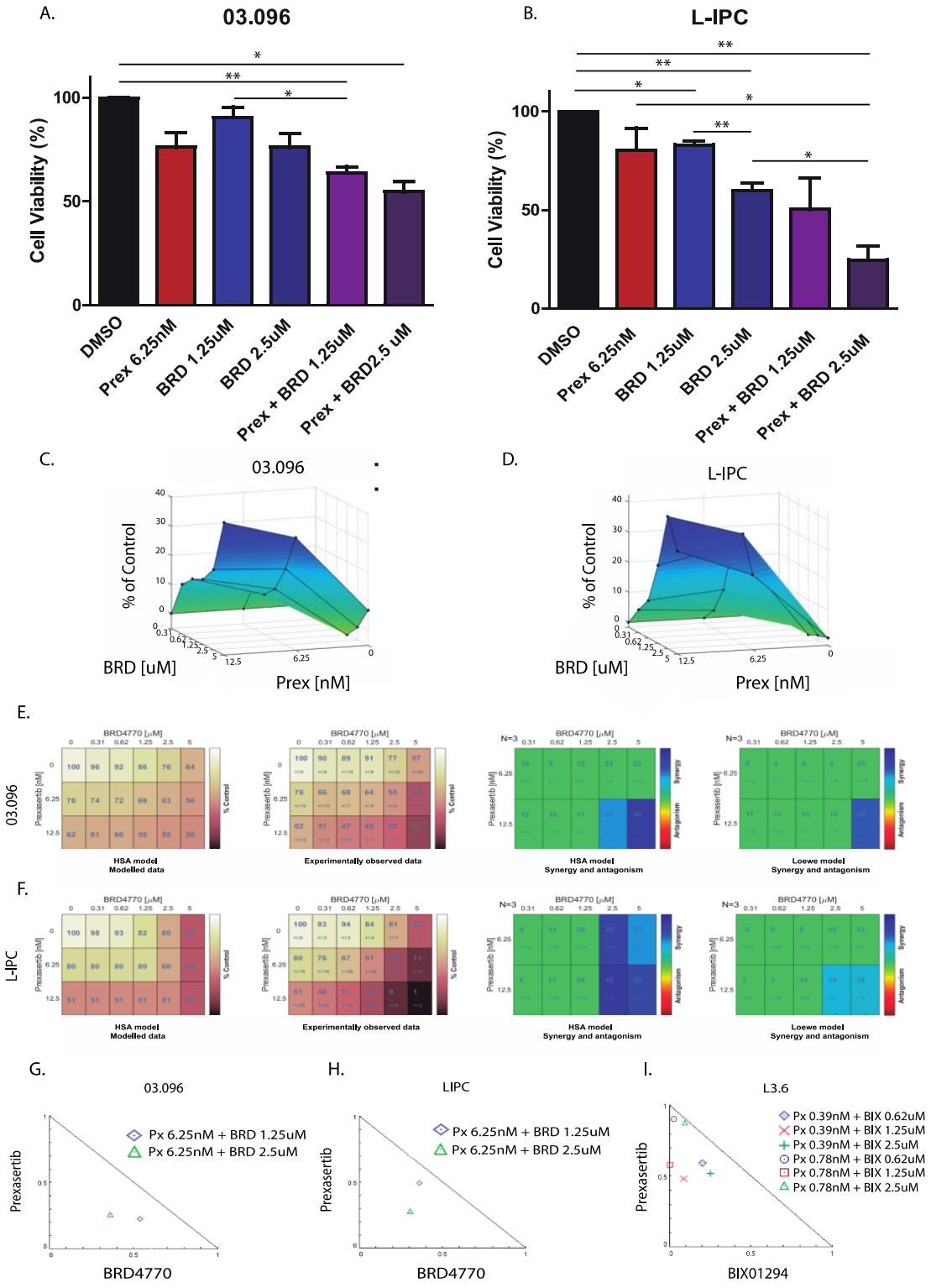

Supplementary Figure 2. CHK1 and G9a inhibition has a synergistic effect on human primary PDAC cell lines. Human primary patient-derived PDAC cell lines were treated with prexasertib (6.25nM) in combination with two doses of BRD4770 (1.25 and 2.5μM). Incucyte

imaging system was used to quantify cell viability. Graph bars show results for (**A**) 03.096 and (**B**) LIPC cells after 72hrs of treatment. Data is expressed as mean±SEM (*, $P<0.05$; **, $P<0.01$; t-test with Welch's correction). 3D representations of calculated pharmacological interactions using Combenefit are shown for (**C**) 03.096 and (**D**) L-IPC cells exposed to the combination of prexasertib and BRD4770 at the indicated doses. Synergistic interactions are shown in blue tones. Modelled and experimental data (first and second panels from left to right) were analyzed independently with the HSA and Loewe synergy models (third and fourth panels) using Combenefit for both (**E**) 03.096 and (**F**) L-IPC cells. In addition, pharmacological interaction was calculated for drug combination at 72hrs using the Chou-Talalay method. Normalized isobolograms for (**G**) 03.096 and (**H**) L-IPC cells show CIs lower than 1, indicating that the drugs act synergistically on human primary PDAC cells. **I,** Compusyn analysis of L3.6 cells treated with another G9a inhibitor, BIX01294 (BIX), in combination with Prex after 72hrs confirms a synergistic interaction.

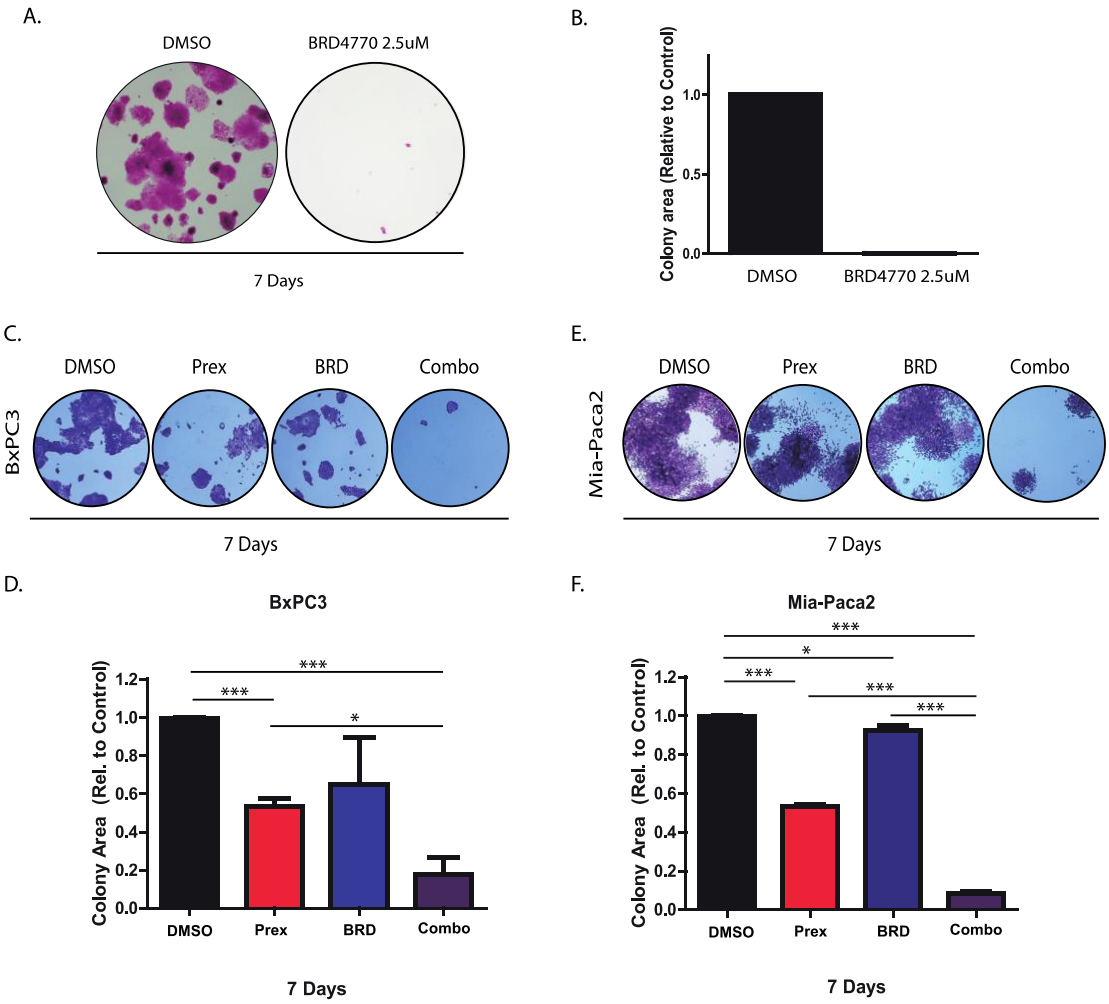

Supplementary Figure 3. Long-term effect of prexasertib and BRD4770 combination treatment demonstrates significant inhibition of cell survival in clonogenic assays. A, Representative images of crystal violet staining from clonogenic survival assays in response to sustained inhibition of G9a (7d) using BRD4770 at 2.5μM demonstrate that this dose eliminated L3.6 colony survival over this time period as an individual treatment, leading to adjustment of doses to assess the combination treatment as presented in Figure 1G-H. **B,** Quantification of colony density relative to control (DMSO) condition is shown. **C**, Clonogenic cell survival assays were also performed on BxPC3 cells. **D**, Graph depicts quantification of colony density, which shows that prexasertib (3.12nM; 53.5±6.6% of control) and BRD4770 (2.5μM; 64.9±24% of control) individually were not as effective at reducing colony survival as in combination (17.4±9.2% of control). **E,** For MiaPaca2 cells, similar effects were observed with clonogenic survival assays. **F,** Graph demonstrates the effect of treatment with prexasertib (6.25nM; 53.3±0.8% of control) or BRD4770 (2.5μM; 92.2±2.8% of control) alone compared to the combination (8.5%±1% of control), which significantly abolishes clonogenic survival. Data is expressed as mean colony density by area relative to control (DMSO) ±SEM (*, *P*<0.05; **, *P*<0.01; ***, *P*<0.001; t-test).

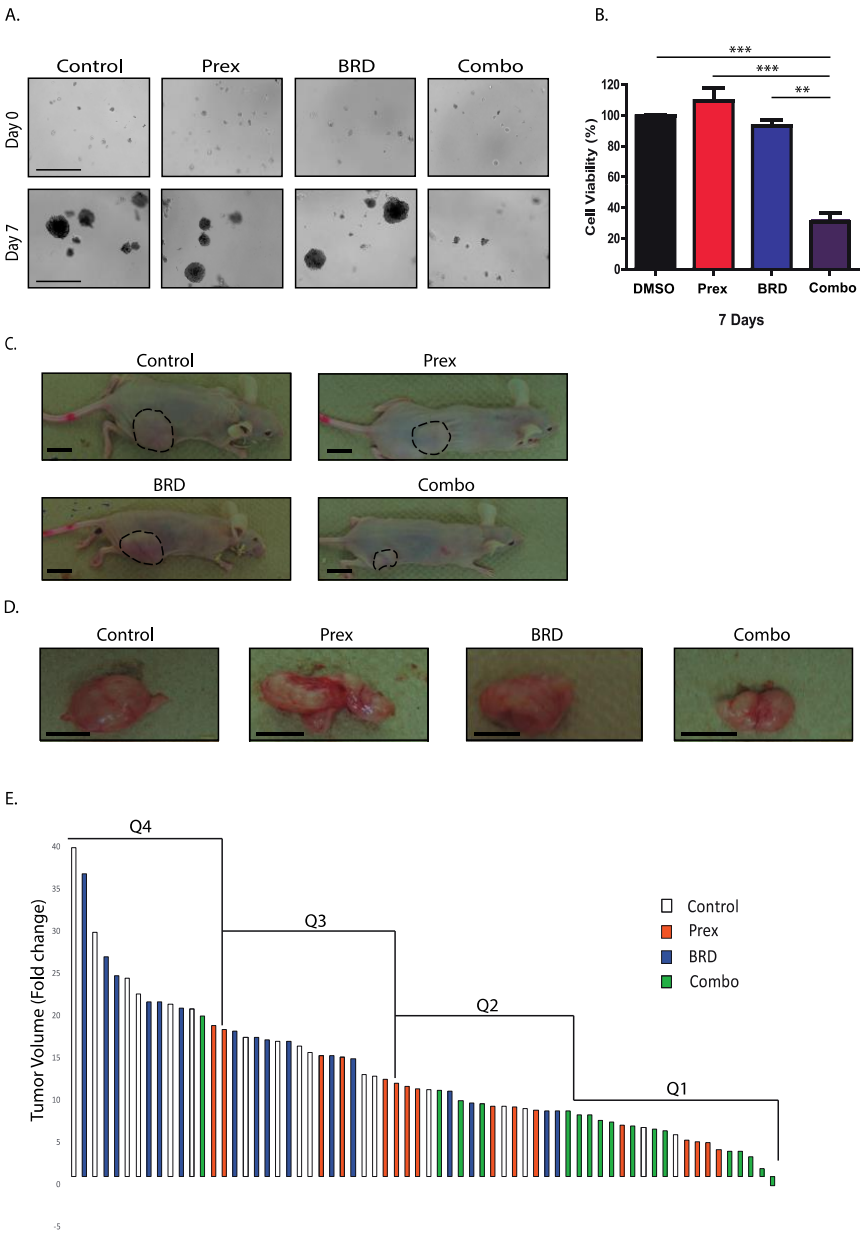

Supplementary Figure 4. Combined prexasertib and BRD4770 treatment is effective *in vivo*. **A,** L3.6 cells grown as 3D spheroids in Matrigel were treated with vehicle control (DMSO), prexasertib (Prex; 1.2nM), BRD4770 (BRD; 2.5µM) or their combination for 7d. **B,** Cell viability was measured by ATP production using CellTiter Glo 3D assay. Graph depicts mean cell viability normalized relative to vehicle-treated control ±SEM (n=3; **, *P*<0.01; ***, *P*<0.001; t-test). **C,** Representative whole-body images of NU/J mice bearing L3.6 xenografts after final treatments. Animals received vehicle treatment (Control), prexasertib (Prex; 2 mg/kg), BRD4770 (BRD; 10 mg/kg) or combination (Combo) during 14d prior to sacrifice. **D,** Representative images of tumors that were harvested after completion of treatments are shown. **E,** Waterfall plot for tumor volume change after 14d of treatment. Bars show tumor fold-change for each animal. Tumors were distributed into 4 quartiles (Q1-Q4), showing combination treatment achieved the overall best responses among the cohorts. (Scale bars, 1cm)

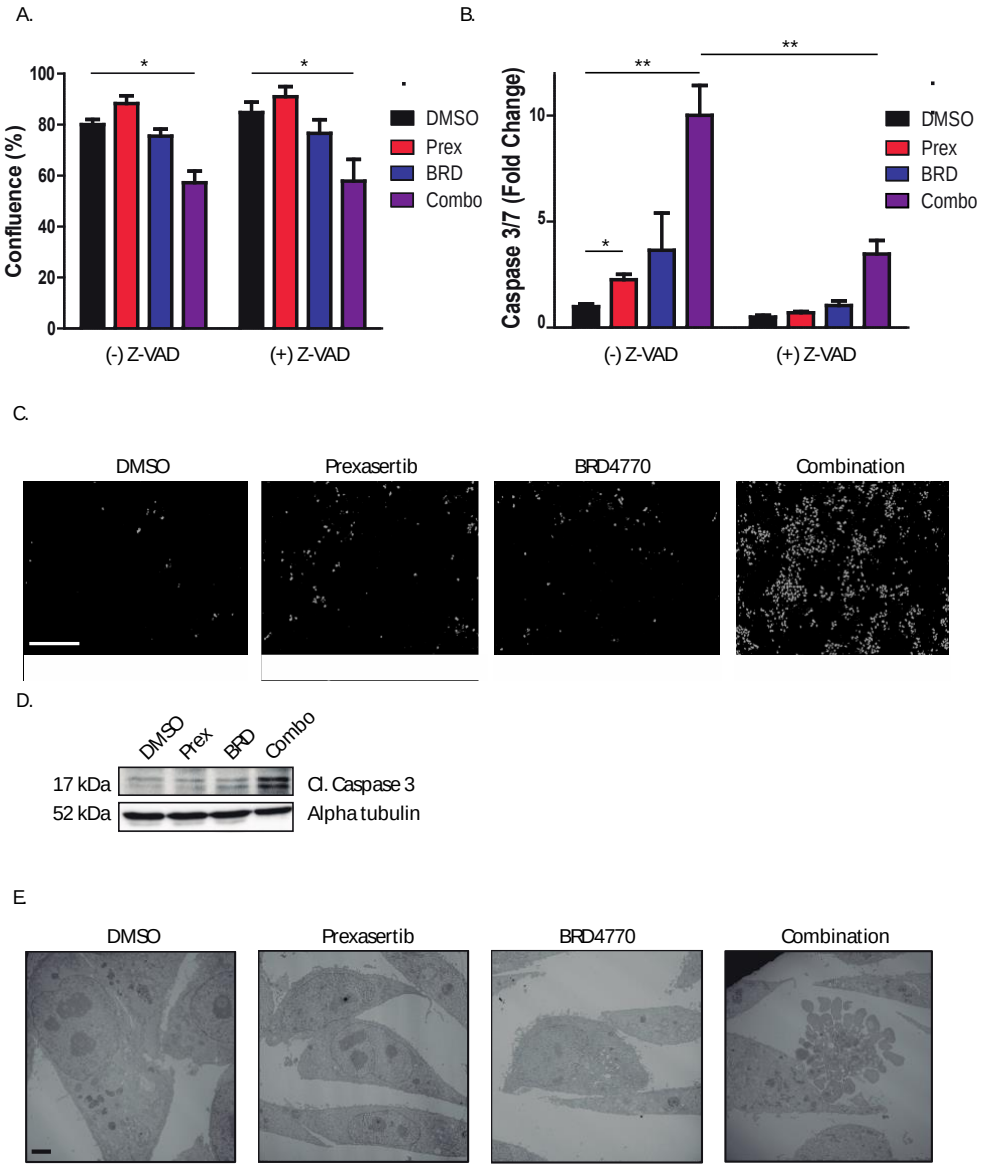

Supplementary Figure 5. Combination treatment induces Caspase 3/7 activation and apoptotic cell death. A, L3.6 cell line was treated with Prexasertib (Prex; 0.78nM), BRD4770 (BRD; 2.5µM) or their combination (Combo) in the absence or presence of the pan-caspase inhibitor Z-VAD-FMK (10µM), and Incucyte live cell analysis of confluence was performed. Mean confluence values ±SEM at 72hrs of treatment are shown. (*, $P<0.05$; t-test) **B,** Graph depicts Caspase 3/7 activation in L3.6 exposed to the aforementioned treatments. Caspase 3/7 signal is shown relative to control (DMSO) after 72hrs of monitoring using the Incucyte imaging system. Mean values ±SEM are shown. (*, $P<0.05$; **, $P<0.01$; t-test) **C,** Representative images from active Caspase 3/7 emitted fluorescence in L3.6 cells following 72hrs of treatment (scale bar, 400µm). **D,** Western blot analysis confirms the cleavage of Caspase 3 as early as 24hrs of combination treatment. **E,** Representative TEM images of L3.6 after 24hrs of treatment. Combination-treated cells show classic morphological traits of apoptosis, including chromatin condensation, micronuclei formation and severe blebbing (scale bar, 2µm).

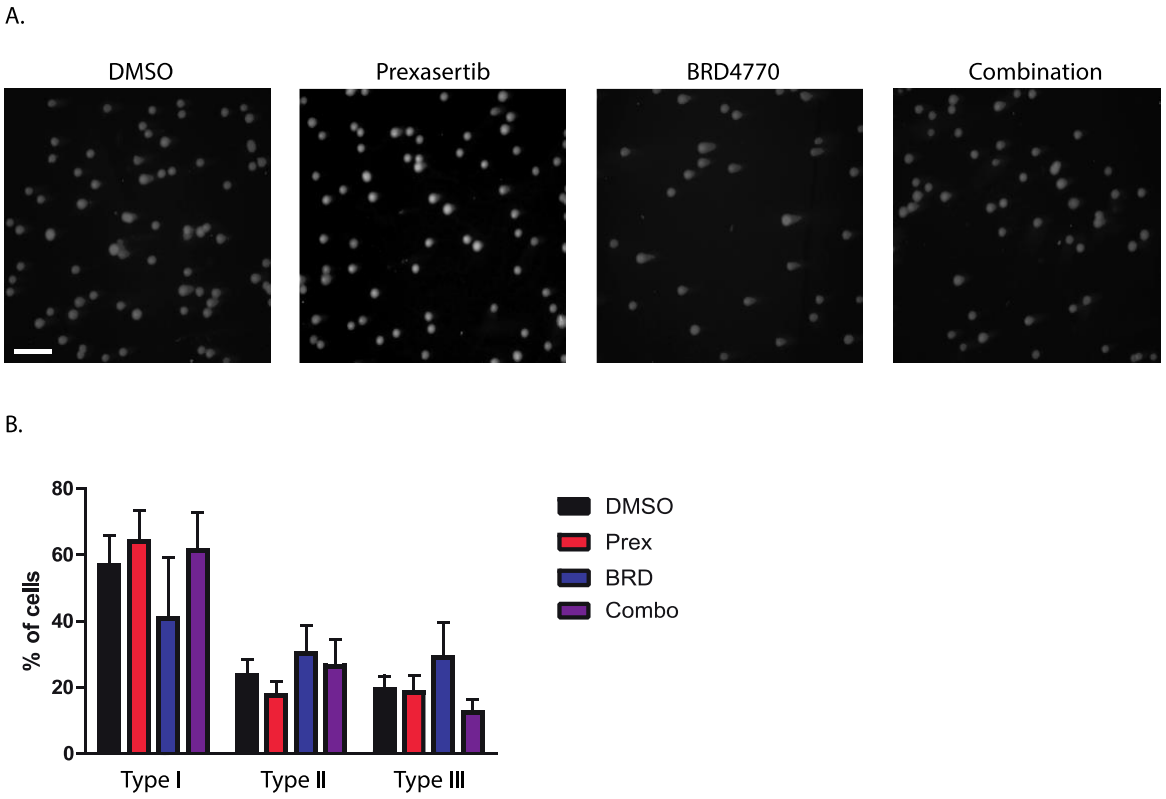

Supplementary Figure 6. Combination treatment does not modify the level of dsDNA breaks in L3.6 cells. A, Representative images from neutral comet assays, indicative of dsDNA breaks, in L3.6 cells treated with Prexasertib (0.78nM), BRD4770 (2.5μM) and their combination after 48hrs are shown (scale bar, 200μm). **B,** Same parameters from Figure 4B were utilized to quantify percentage of treated cells distributed into Type I, II and III of dsDNA damage. Graph shows the mean±SEM. Unlike the results from the alkaline comet assay (Figure 4A-B), which detects ssDNA and dsDNA breaks, there are no significant differences among conditions for dsDNA breaks alone, indicating that the majority of observed DNA damage consists of ssDNA breaks. (P>0.05; t-test)

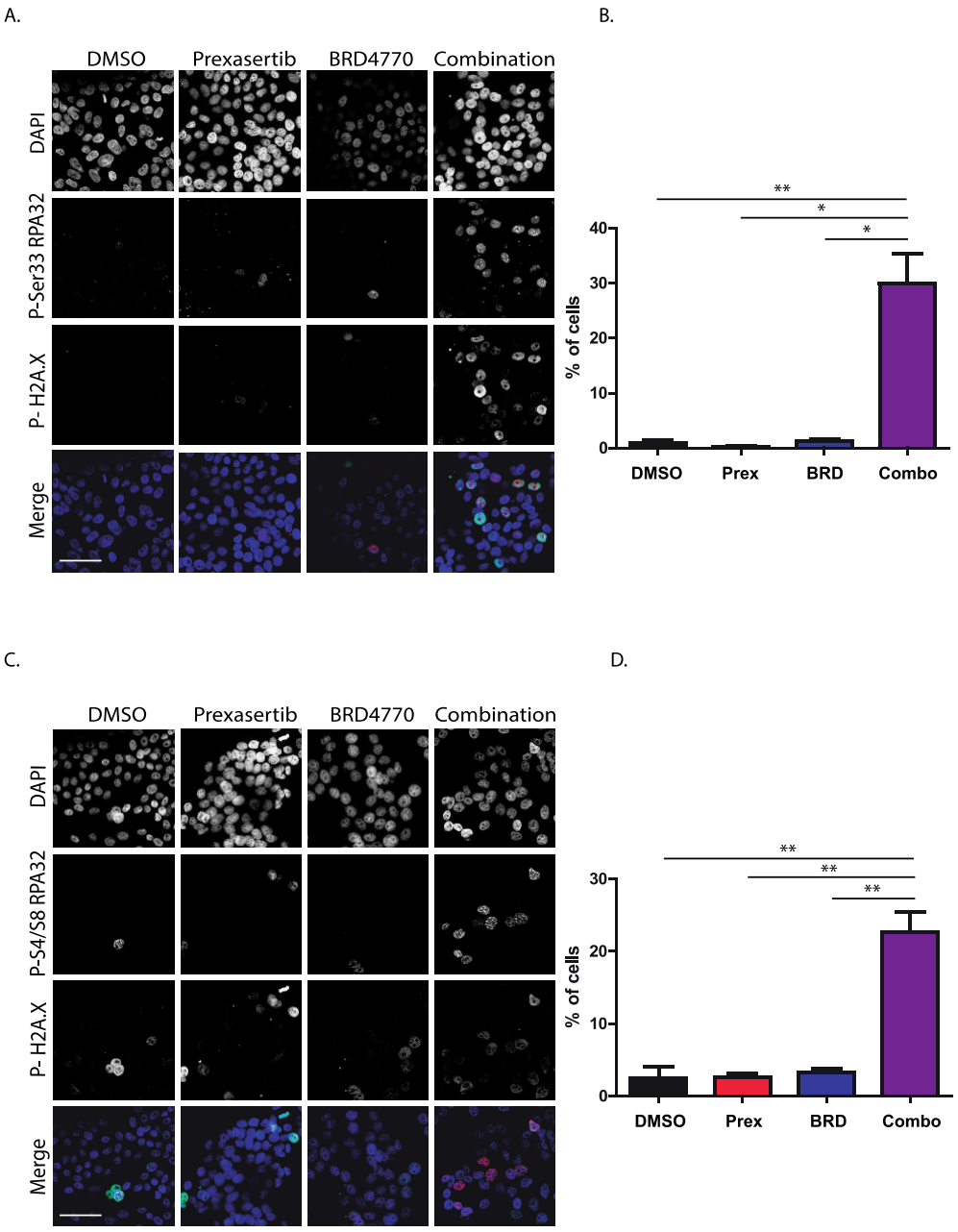

Supplementary Figure 7. Combined CHK1 and G9a inhibition induces phosphorylated RPA32 and H2A.X double-positive cells. L3.6 cells treated with Prexasertib (0.78nM), BRD4770 (2.5μM) or combination for 24hrs were co-stained for P-Ser33-RPA32 (red) and P-Ser139-H2A.X (green) with DAPI DNA counterstain (blue). **A,** Representative confocal micrographs for all conditions are shown (scale bar, 50μm). **B,** Cells positive for both marks were quantified and expressed in the graph as the mean±SEM (*, *P*<0.05; **, *P*<0.01; t-test with Welch's correction). L3.6 cells treated under the same conditions for 24hrs were also co-stained for P-S4/S8-RPA32 (red) and P-Ser139-H2A.X (green). **C,** Representative confocal micrographs for all conditions are shown (scale bar, 50μm). **D,** Double-positive cells were quantified, and the mean±SEM is depicted in the graph (*, *P*<0.05; **, *P*<0.01; t-test).

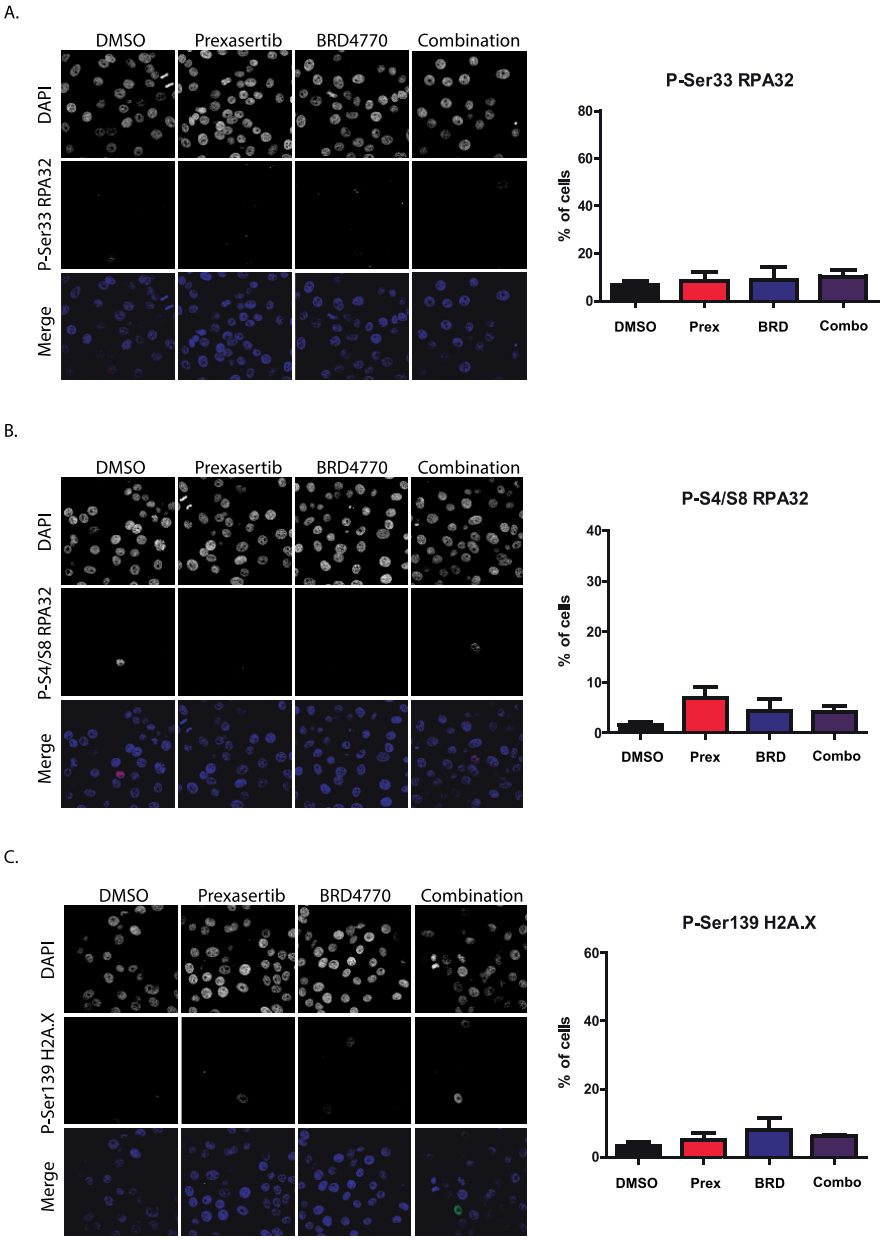

Supplementary Figure 8. Synergistic effect is not observed with predicted non-synergistic concentrations of prexasertib and BRD4770. Based on immunostaining data presented in Figure 5, modelled and experimental data were analyzed independently with the HSA and Loewe synergy models with Combenefit software, and a non-synergistic pharmacological interaction was predicted for a combination of prexasertib at 0.39nM and BRD4770 at 1.25µM. Immunostaining for P-Ser33-RPA32 (**A**), P-S4/S8-RPA32 (**B**), and P-Ser139-H2A.X (**C**) was repeated with these predicted non-synergistic concentrations as a negative control. L3.6 cells were treated for 24hrs with prexasertib (0.39nM) and BRD4770 (1.25µM) alone and in combination. Cells positive for P-Ser33-RPA32, P-S4/S8-RPA32, and P-Ser139-H2A.X were quantified as Mean±SEM, demonstrating that, unlike the synergistic concentrations (shown in Figure 5), the non-synergistic doses of prexasertib and BRD4770 do not change level of these markers (n=3; *P*>0.05; ANOVA).